Comparison of 3D transitional CFD simulations for rotating wind turbine wings with measurements

Paper

Schaffarczyk, A P; Boisard, R; Boorsma, K; Dose, B; Lienard, C; Lutz, T; Aagaard Madsen , Helge; Rahimi, H; Reichstein, T; Schepers, G; Sørensen, Niels N.; Stoevesandt, B; Weihing, P

Published in:
Journal of Physics: Conference Series

Link to article, DOI:
10.1088/1742-6596/1037/2/022012

Publication date:
2018

Document Version
Publisher's PDF, also known as Version of record

Comparison of 3D transitional CFD simulations for rotating wind turbine wings with measurements

IOP Conf. Series: Journal of Physics: Conf. Series **1037** (2018) 022012 doi:10.1088/1742-6596/1037/2/022012

Comparison of 3D transitional CFD simulations for rotating wind turbine wings with measurements

A P Schaffarczyk[6,8], R Boisard[7], K Boorsma[2], B Dose[3,4], C Lienard[7], T Lutz[5], H Å Madsen[1], H Rahimi[3,4], T Reichstein[6], G Schepers[2], N Sørensen[1], B Stoevesandt[4] and P Weihing[5]

[1] DTU Wind Energy, Roskilde and Lyngby, Denmark
[2] ECN, Petten, The Netherlands
[3] ForWind, Institute of Physics, University of Oldenburg, Oldenburg, Germany
[4] Fraunhofer IWES, Oldenburg, Germany
[5] Institute of Aerodynamics and Gas Dynamics, University of Stuttgart, Stuttgart, Germany
[6] Kiel University of Applied Sciences, Kiel, Germany
[7] ONERA, The French Aerospace Lab, Palaiseau, France
[8] corresponding author

E-mail: `Alois.Schaffarczyk@fh-kiel.de`

Abstract. Since the investigation of van Ingen *et al.*, attempts were undertaken to search for laminar parts within the boundary layer of wind turbines operating in the lower atmosphere with much higher turbulence levels than seen in wind tunnels or at higher altitudes where airplanes usually fly. Based on the results of the DAN-Aero experiment and the Aerodynamic Glove project, a special work package *Boundary Layer Transition* was embedded in IAEwind Task 29 *MexNext* 3rd phase (MN3). Here, we report on the results of the application of various CFD tools to predict transition on the MEXICO blade. In addition, recent results from a comparison of thermographic pictures (aimed at detecting transition) with 3D transitional CFD are included as well. The MEXICO (2006) and NEW MEXICO (2014) wind tunnel experiments on a turbine equipped with three 2.5 m blades have been described extensively in the literature. In addition, during MN3, high-frequency Kulite data from experiments were used to detect traces of transitional effects. Complementary, the following set of codes were applied to cases 1.1 and 1.2 (axial inflow with 10 m/s and 15 m/s respectively) – elsA, CFX, OpenFOAM (with 2 different turbulence/transitional models), Ellipsys, (with 2 different turbulence models and e^N transition prediction tool), FLOWer and TAU – to search for detection of laminar parts by means of simulation. Obviously, the flow around a rotating blade is much more complicated than around a simple 2D section. Therefore, results for even integrated quantities like thrust and torque are varying strongly. Nevertheless, visible differences between fully turbulent and transitional set-ups are present. We discuss our findings, especially with respect to turbulence and transition models used.

1. Introduction

This paper focuses on the results of work conducted in subtask 4.9 *Boundary layer transition* of IEA Wind Task 29 MexNext. Participants were: DTU Wind Energy (Denmark), ONERA (France), Fraunhofer IWES/ForWind, Oldenburg, IAG/U Stuttgart and UAS Kiel (Germany). Previous work on this subject is summarized in table 1.

Table 1. Previous work on boundary layer investigations on 3D rotating wind turbine blades.

Name of Project	Date	Remark	Source
HAT25	1983	Transition detection via microphone	[1]
MEXICO	2006 and 2013	PIV and Kulite data	[2]
DAN-Aero	2007 - 2009	Full Scale LM 38.8	[3]
Aerodynamic Glove	2011	Enercon 33 with 15 m blade	[4]
AVATAR	2011 - 2017	DU00-W-212 profile	[5]
Free Field Thermography	2014 - 2016	LM37 (meter) blade	[6]

The paper is organized as follows: We shortly compare our 3D case to a recent but simpler 2D case and summarize recent findings from re-anlysis of experimental high-frequency pressure measurements. Then, we present the main work of 3D computations starting with global force- and torque-data but include some more detailed results concerning radial resolved pressure and wall-shear stress. Finally, we discuss another comparison concerning transition with thermographic pictures of a larger wind turbine.

2. Boundary Layer Transition on Rotating Wind Turbines

Due to renewed interest in boundary layer experiments of wind-turbine blades operating in the free atmosphere [1, 3, 4, 7, 8] a work-plan to investigate these issues on the MEXICO blade was released in the beginning of 2013 within MN2 (2012 - 2014) but most of the work was performed in MN3 (2015 - 2017) only.

A set of measurements without and with only partially tripped blades were performed during the NewMexico experiment and were reported in 2014 [9, 10, 11].

Recently, for a two-dimensional setup during the EU-funded AVATAR project (see [13]), remarkable consistent findings were reported for predicting c_L and c_D data using transition predicting tools like e^N [14] or Menter's correlation based model [15]. The Reynolds number (RN) was varied from 3 to 12 mio and the turbulence intensity (TI) ranged from about 0.086 % to 0.5 %. Fig. 1 shows the importance of incorporating the turbulence intensity for choosing an appropriate N and Fig. 2 shows the differences of various methods and codes used for one specific case (RN = 15 mio and TI = 0.33 %). In all transitional cases Mack's correlation

$$N = 2.13 - 6.18 \cdot \log(TI) \tag{1}$$

was used to correlate TI and N. In contrast to applications for pure 2D flows for aiRFOILs measured in wind tunnels, complete 3D transitional simulations, especially for rotating wings, are much more rare and more complicated to simulate as well.

2.1. Experiments on Rotating Wind Turbine Blades

The earliest approach of searching for traces of laminar-turbulent transition on a rotating wind turbine blade dates back to 1983 [1, 16]. The then used blade had a length of 14 m and profiles from the NACA 4-digit 44 series were used. Rated power of this turbine was 300 kW. The Reynolds number varied from 1 to 3 mio. One main finding was the safe detection of laminar parts even under apparently high inflow turbulence.

Years later in Denmark [3, 17], a MultiMW (Nec Micon NM80 with LM38 blades) was investigated in much more detail. Due to much faster signal-processing capabilities much sharper detection of transition locations was possible and even changes during one revolution ($T \approx 5$ sec)

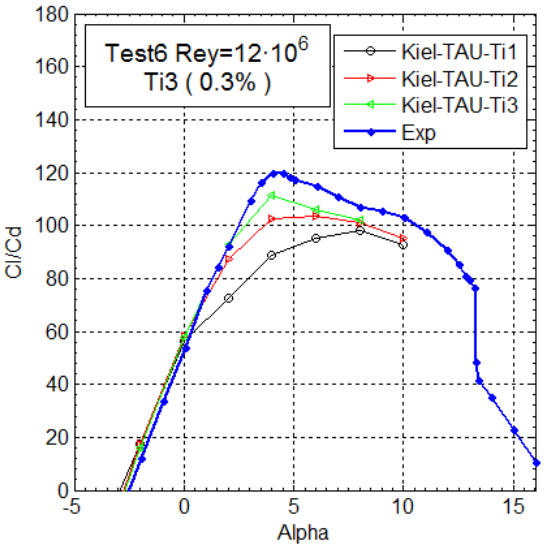

Figure 1. Comparison of CFD and experimental data: Lift-to-drag ratio vs. angle of attack (AOA) for different turbulence intensities (Ti1 = 2.39 %, Ti2 = 0.55 % and Ti3 = 0.33 %). *Kiel-TAU* refers to the TAU code from DLR [12] as applied by University of Applied Sciences Kiel [5].

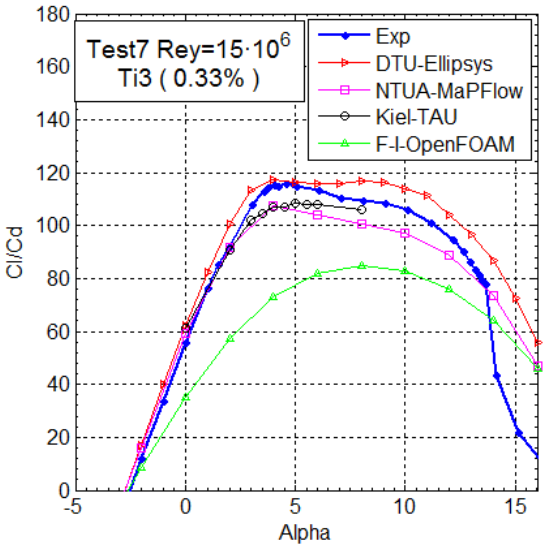

Figure 2. Comparison of experimental data with CFD results for various CFD codes and methods [5].

could be detected. There, one major finding was the observation of pronounced laminar parts (20 % to 40 % with regard to x/c) and that the energy increase within the turbulent boundary layer starts above approximately 500 Hz. This explains that even under seemingly much higher turbulent inflow, only a small part is *aerodynamically active*. If one assumes the mechanism of *receptivity* as responsible, then a low-frequency cut-off may exist.

Partially, this was confirmed by the *Aerodynamic Glove* experiment [4] performed on ENERCON E30 with 15 m blades, in size rather comparable to the much older HAT25 experiment [16]. It was found that the energy content (of the turbulent atmosphere) in a frequency range above 0.5 kHz is about 6 orders of magnitude smaller than at its maximum at about 10^{-2} Hz. This then justified using a N-factor of $N = 8$, corresponding to $TI = 0.11\%$ for CFD. Due to the different sensor type used (hot films instead of microphones) only a very limited range ($0.24 \leq x/c \leq 0.31$) in chordwise direction could be screened. Nevertheless, some of the over 700 recorded data-sets clearly showed transition detected by the same type of reasoning and criteria as used above in the DAN-AERO experiment [3, 17].

2.2. Results from Re-Analysis of NEW MEXICO Kulite data

NEW MEXICO data, especially the high-frequency Kulite data has been re-processed by Lobo [18, 19] for possible detection of transition by comparing the energy content in various frequency ranges. He found (see Fig. 3) a rather similar dependency if all measurements were collapsed to one graph by relating them to their corresponding angle of attack calculated with the help of RFOIL. As can be seen in Figs. 8 and 9, his method also compares well with CFD simulations.

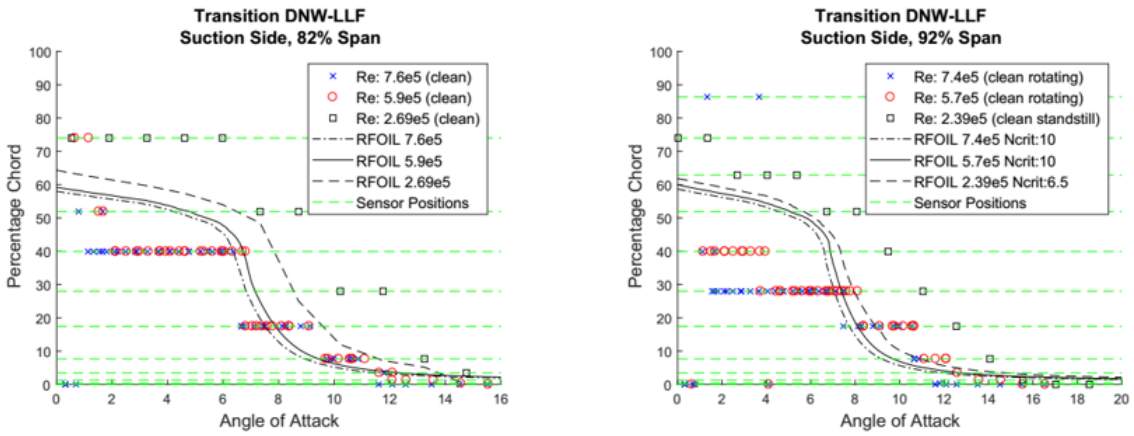

Figure 3. Locations of transition from analyzing Kulite data. Both rotating and standstill conditions are included [18].

2.3. CFD comparison of NEW MEXICO experimental data

2.3.1. Overview of CFD Codes A short overview of the used codes (elsA, CFX, EllipSys, FLOWer, OpenFOAM and TAU) is given. For more details, see the comprehensive summary of MN3 [20] and references therein, especially appendix F and section 4.4 *Convergence of CFD simulations*.

Three of the codes come from aerospace research institutions: elsA from ONERA (France) and FLOWer and TAU from DLR (Germany). CFX [21] is the only commercial code used (ANSYS), EllipSys was developed by the Danish Technical University and OpenFOAM by the openFOAM community [22]. All have been tested and validated extensively and represent state of the art RANS-CFD codes. Mesh size ranges from 15 mio (CFX) to 140 mio (elsA) and the computational domain from 5 rotor diameters (elsA) to 30 rotor diameters (TAU). As the turbulence model, SST-k-ω was used in almost all cases. The number of revolutions varied from 10 (TAU) to 30 (elsA).

2.3.2. Global results for thrust and torque During MexNext Phase 3, many (some of them new) codes were able to perform simulations. Table 2 summarizes the results for thrust and torque for cases 1.1 (10 m/s inflow velocity) and 1.2 (15 m/s inflow velocity). Given are the results for fully turbulent CFD simulations, transitional CFD simulations and experimental data, respectively. Table 3 summarizes the averages of all contributions and indicates general deviations from the different methods.

It should be noted that the measurements from 2014 seem to be somewhat more reliable because some systematic errors from the 2006 run could be identified and corrected as described in [23].

2.3.3. Radially resolved data In a next step – to have more insight into the reasons of the variations in global forces – the radially resolved data were compared. Figs. 4 and 5 give an impression of the calculated deviations (fully turbulent vs. transitional) of tangential forces from some arbitrary chosen groups (DTU, ONERA IWES/ForWind and U Stuttgart). Transitional and turbulent data are rather close inside one group but differ significantly, however. Especially at $1 \leq r \leq 1.5$, large differences are visible due to a change in airfoil type and interrupted tripping [18].

Table 2. Global results for thrust (N) and torque (Nm)

fully turbulent CFD

Year	Code	Thrust case 1.1	Torque case 1.1	Thrust case 1.2	Torque case 1.2
2010	EllipSys	1000	70	1550	370
2016	EllipSys	969	59	1704	278
2012	TAU (Kiel)	1036	30	1608	220
2015	TAU (DLR)	1050	75	1800	360
2016	elsA	1064	32	1781	295
2017	OpenFOAM SA	937	70	1667	338
2017	OpenFOAM SST	979	73	1749	343
2017	FLOWer	920	77	1725	350

transitional CFD

	Code	Thrust case 1.1	Torque case 1.1	Thrust case 1.2	Torque case 1.2
	elsA	1086	33	1791	302
	CFX	840	50	1790	250
	FLOWer	953	81	1793	357
	OF kkL omega	1047	85	1875	364
	OF gamma Re	990	76	1729	333
	EllipSys [23]	984	58	1752	278
	TAU	1025	74	1800	465

experimental data

Year	Experiment	Thrust case 1.1	Torque case 1.1	Thrust case 1.2	Torque case 1.2
2006	MEXICO	854	61	1517	285
2014	NEW MEXICO	974	68	1663	301

2.3.4. Impact on pressure distribution In Fig. 6, the pressure on the first downstream half of the suction side is shown for comparison. Even from this graph, a clear indication (as sudden change in slope at z $\sim$ 0.02 m and z $\sim$ 0.035 m, respectively) where transition takes place can be deduced: $z_{tr} \approx 0.02$ m for the ONERA simulation and $z_{tr} \approx 0.035$ m for DTU. In general – as expected – both transitional pressure distributions give raise to more lift than in the fully turbulent case.

2.3.5. Impact on wall shear stress distribution For more insight into the details of a transitional simulation, the local friction coefficient c_f is shown in Fig. 7. Usually, in CFD simulations transition (i.e. switching-on of the used turbulence model) is blended by an *intermittency* function over a well defined finite region.

This can be clearly seen in the figure, although the location itself is different. As the fully

Table 3. Comparison of averages (AVR) and standard deviation (STD) for thrust (N) and torque (Nm) at 10 m/s and 15 m/s inflow. N is the number of data points or different computational runs. Values in brackets for experimental data are from NEW MEXICO.

type	velocity (m/s)	Thrust AVR	Thrust STD	Torque AVR	Torque STD
Experiment	10	914 (974)	42	65 (68)	2
N = 2	15	1590 (1663)	52	301 (317)	11
fully turbulent	10	998	17	60	6
N = 8	15	1697	42	305	20
transitional	10	983	26	62	7
N = 7	15	1790	15	337	26

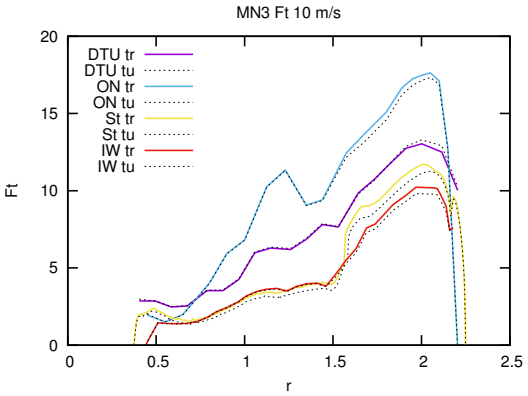

Figure 4. Radially resolved tangential force (in N/m) from fully turbulent and transitional CFD calculations, case 1.1: 10 m/s inflow.

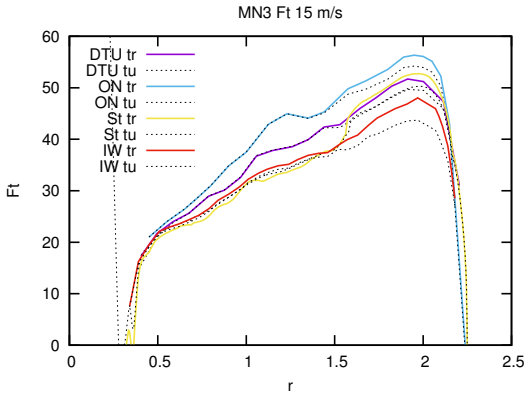

Figure 5. Radially resolved tangential force (in N/m) from fully turbulent and transitional CFD calculations, case 1.2: 15 m/s inflow.

turbulent region starts from c_f^{max}, differences here only stem from the used turbulence and prediction models. ONERA uses a Menter-Langtry criterion [25] and IWES/ForWind uses $\gamma - Re_\theta$. The laminar part (up to c_f^{min}) however, should be identical – or at least very similar – if mesh and boundary conditions would be the same. Experimental data (Figs. 8 and 9) from Lobo [18] support this reasoning.

It is clearly seen that the results for the suction side ($x_{tr}^{suc,CFD} = 0.16 \ldots 0.45$) vary more than for the pressure side ($x_{tr}^{pres,CFD} \approx 0.6$). From Fig. 8, one finds $x_{tr}^{suc,exp} = 0.2 \ldots 0.3$ and from Fig. 9 $x_{tr}^{pres,exp} = 0.7$ is estimated. With some caution, a reasonable agreement between measurements and CFD simulations can be found.

2.4. Transition on a 37 m blade

In addition to the MexNext project, the TAU code was used to simulate 3D transition on a 37 m blade at partial load. For this specific blade thermographic images exist [6]. The comparison of thermographic images with CFD simulations [26] showed a discrepancy in the position of the laminar-turbulent transition. Thus, in this case it is not possible to confirm the large extension

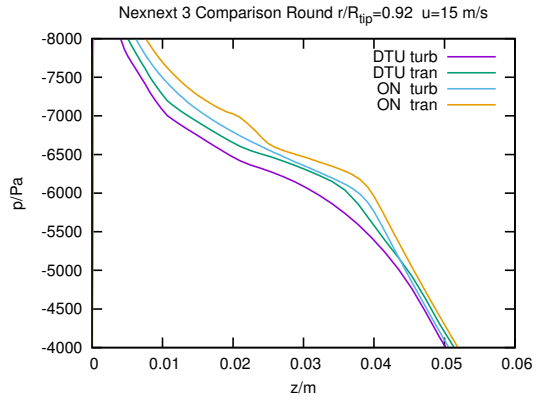

Figure 6. Pressure distribution on (the first part of) the suction side from fully turbulent and transitional CFD calculations. Data kindly provided by DTU and ONERA.

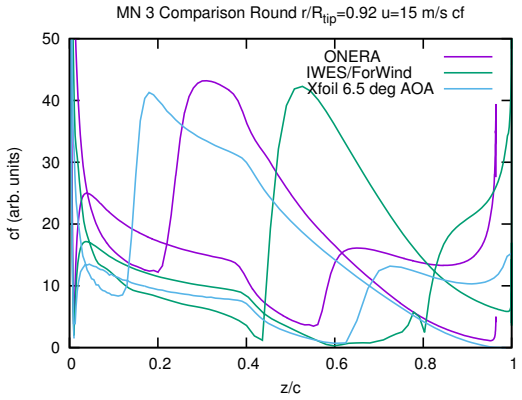

Figure 7. Prediction of c_f for location of transition (first minimum) from CFD. Both pressure and suction sides are included. For comparison, an XFOIL [24] calculation with estimated AOA of 6.5 deg is added. Data kindly provided by IWES/ForWind and ONERA.

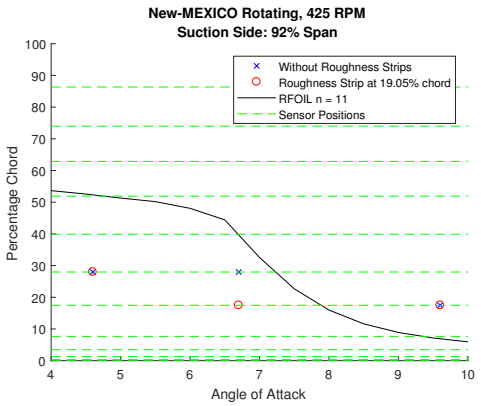

Figure 8. Locations of transition from analyzing Kulite data for the same case as in Fig. 7, suction side.

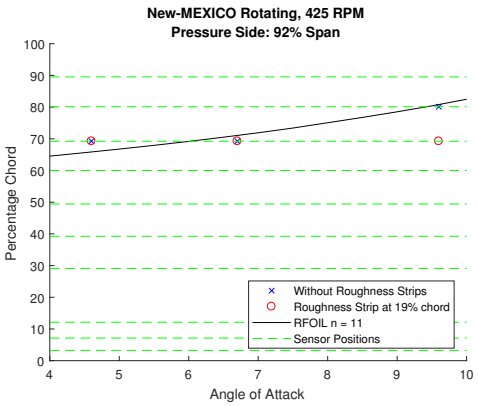

Figure 9. Locations of transition from analyzing Kulite data for the same case as in Fig. 7, pressure side.

of an assumed laminar state (more than 40 % relative chord along almost the whole blade) by this specific transition prediction tool. However, some of the operating conditions of the turbine, e.g., wind velocity and pitch angle, were not known accurately. Therefore, it might be possible that the optical findings can be reproduced with appropriate simulation parameters.

3. Summary, Discussion and Conclusions

During the 3rd period of IEA Wind Task 29 *MexNext*, seven transitional CFD calculations from four groups (DTU, IWES/ForWind, Onera, U Stutt and UAS Kiel) were able to perform 3D transitional CFD computations. In addition, high frequency pressure data was re-processed and transition locations could be deduced which agree reasonably with RFOIL and 3D transitional RANS simulations. For a special case (see section 2.3.5), a detailed comparison of measurements and simulations show reasonable agreement.

Due to decambering and larger turbulent wall shear stress it was expected that transitional simulations should give slightly larger integrated force values at non-tripped outboard sections. This is easily confirmed even by a simple XFOIL estimation for the r/R_{tip} =92% section at Re = 1 mio and an assumed AOA of 6°: Lift increases from 0.96 to 1.06 and drag is reduced from 0.015 to 0.009. As it is typical for XFOIL, the transition location is visible as a cusp in c_p. Comparable cusps at z = 0.02 m seem to be present in Fig. 6 for ONERA transitional case 1.2.

Finally, the following more specific conclusions may be drawn separately for the two different cases:

- inflow 10 m/s (case 1.1, TSR = 10):
  Transitional thrust and torque agree (within the statistical standard deviation (std) obtained from all computational runs) with the experiment and fully turbulent flow. An expected increase of force/moment data is barely visible.
- inflow 15 m/s (Case 1.2, TSR = 7):
  Both thrust and torque statistically increase significantly if transition is enabled but seem to depart from the experimental values even further.

In conclusion, it has to be noted that 3D transitional CFD simulations do not have the consistency of 2D results obtained, e.g., from the recently finished AVATAR project as described in Ref. [5]. In general, our data (for integrated thrust and torque) show approximately the same scattering as in previously obtained other computational rounds.

As an outlook, efforts should be undertaken as proposed by [27]. As a first step, it may be appropriate to use identical meshes to investigate exclusively the effects of the transition-predicting modules only. However, turbulence and transitions modules are known to be very sensitive to mesh parameter and, as a result may prevent using a unique mesh for all solvers.

Acknowledgments

The authors Schaffarczyk and Reichstein acknowledge the North-German Supercomputing Alliance (HLRN) for providing HPC resources that have contributed to the research results reported in this paper.

References

[1] van Ingen J L and Schepers J G 2012 "Prediction of boundary layer transition on the wind turbine blades using the eN method and a comparison with experiment", *Private communication*
[2] Schepers J G and Snel H 2007 Energy Research Centre of the Netherlands Report ECN-E–07-042
[3] Madsen, H et al. 2010 48th AIAA Aerospace Science Meeting Including the New Horizons Forum and Aerospace Exposition, 4 – 7 Jan 2010, Orlando, Florida (AIAA 2010-645)
[4] Schaffarczyk A P, Schwab D and Breuer M 2016 *Wind Energy* **20** 211
[5] Ceyhan, O et al. 2017 35th Wind Energy Symposium, 9 – 13 Jan 2017, Grapevine, Texas (AIAA 2017-0915)
[6] Balaresque N et al. 2016 *J. Phys.: Conf. Series* **753** 072012
[7] Schaffarczyk A P, Schwab D, Ingwersen S and Breuer M 2014 *J. Phys.: Conf. Series* **555** 012092
[8] Schaffarczyk A P 2014 *Introduction to Wind Turbine Aerodynamics* (Berlin: Springer)
[9] Cho T and Kim C 2014 *Renewable Energy* **65** 265
[10] Schepers J G and Boorsma K 2014 Energy Research Centre of the Netherlands Report ECN–E-14-048
[11] Boorsma K 2014 *Mexnext Progress overview* MexNext IEA Task 29 Meeting, 29 – 31 Oct 2014, Mianyang, China
[12] TAU-Code User Guide, Release 2014.2.0 2014
[13] `www.eera-avatar.eu`
[14] van Ingen, J 2008 38th Fluid Dynamics Conference and Exhibit, 23 – 26 Jun 2008, Seattle, Washigton (AIAA 2008-3830)
[15] Menter F R, Langtry R B, Likki S R, Suzen Y B, Huang P G and Völker S 2004 *J. Turbomach.* **128** 413
[16] van Groenewoud G J H, Boermans L M M and van Ingen J L 1983 Delft University of Technology Report LR-390
[17] Troldborg N, Bak C, Aagaard Madsen H and Skrzypinski W R 2013 *DANAERO MW: Final Report* Technical University of Denmark Report DTU Wind Energy E-0027(EN)

[18] Lobo B 2018 *Investigation into Boundary Layer Transition on the MEXICO Blade* University of Applied Sciences Flensburg MSc Thesis, available on request as ECN-WIND-2018-006
[19] Lobo B 2018 *Investigation into Boundary Layer Transition on the MEXICO Blade* The Science of Making Torque from Wind, 20 – 22 Jun 2018, Milan, Italy
[20] Boorsma K et al. 2018 Energy Research Centre of the Netherlands Report ECN–E-18-003
[21] Rathje T 2016 *CFD-Untersuchungen am MEXICO Flügel mit CFD* University of Applied Sciences Kiel BEng thesis (in German), available on request from UAS Kiel
[22] `www.openfoam.com`
[23] Sørensen N N, Zahle F, Boorsma K and Schepers G 2016 *J. Phys.: Conf. Series* **753** 022054
[24] Drela M 1989 *XFOIL: An Analysis and Design System for Low Reynolds Number Airfoils,* In: *Low Reynolds Number Aerodynamics* ed. Mueller T J (Berlin: Springer) p. 1–12
[25] Lienard C and Boisard R 2018 2018 Wind Energy Symposium, 8 – 12 Jan 2018, Kissimmee, Florida (AIAA 2018-1495)
[26] Mommsen K 2017 *3D Laminar-Turbulent Transition on Wind Turbine Blades by CFD* University of Applied Sciences Flensburg MSc thesis, available on request from UAS Flensburg
[27] Gomez-Iradi S, Herraez I, Sørensen N and Weighin P 2017 *Simulation convergence MexNext 3* MexNext Phase 3 intermediate meeting, Pamplona, Spain